Chirped pulse formation dynamics in ultra-long mode-locked fiber lasers

E. J. R. Kelleher[1,*] and J. C. Travers[2]

[1]*Femtosecond Optics Group, Department of Physics, Imperial College London, Prince Consort Road, London SW7 2AZ, UK*

[2]*Max Planck Institute for the Science of Light, Guenther-Scharowsky-Strasse 1, 91058 Erlangen, Germany*

**Corresponding author: edmund.kelleher08@imperial.ac.uk*

Received November 25, 2013; revised January 24, 2014; accepted January 24, 2014;
posted January 27, 2014 (Doc. ID 201973); published March 5, 2014

By modeling giant chirped pulse formation in ultra-long, normally dispersive, mode-locked fiber lasers, we verify convergence to a steady-state consisting of highly chirped and coherent, nanosecond-scale pulses, which is in good agreement with recent experimental results. Numerical investigation of the transient dynamics reveals the existence of dark soliton-like structures within the envelope of the initial noisy pulse structure. Quasi-stationary dark solitons can persist throughout a large part of the evolution from noise to a stable dissipative soliton solution of the mode-locked laser cavity. © 2014 Optical Society of America

OCIS codes: (190.5530) Pulse propagation and temporal solitons; (190.4370) Nonlinear optics, fibers; (140.4050) Mode-locked lasers; (190.3100) Instabilities and chaos; (190.5940) Self-action effects.

http://dx.doi.org/10.1364/OL.39.001398

Lasers have long proven a convenient experimental platform for the fundamental study of wave dynamics. Perhaps the most celebrated conceptual connection is that of the optical rogue wave [1–3], which might lead to an improved understanding of the mechanisms involved in the formation of freak, large-amplitude ocean waves. Recently, another hydrodynamics analogy has been drawn between the breakdown of temporal coherence in a fiber laser and the onset of turbulent fluid flow [4]. The precursor to the turbulent regime was identified as bunching and multiple collisions between dark and gray temporal solitons arising from the continuum in the presence of nonlinearity and normal dispersion.

In a fiber laser, a reduction in temporal coherence arises due to a dephasing between the large number of allowed cavity modes involved in laser action. Long-range order of the mode population in a quasi-continuous-wave (CW) fiber laser can be imposed by the inclusion of a saturable absorber element, leading to the generation of a regular train of mode-locked pulses in the time-domain [5]. Recently, a trend toward elongation of the cavity in a fiber laser has been partially driven by the need for higher pulse energies, but mostly out of curiosity as to the limit of ultra-long pulse and low repetition rate mode-locked fiber lasers [6–8]. In particular, adopting purely normal cavity dispersion—supporting dissipative soliton solutions—has proven the most robust, while offering the highest degree of power scalability. Yet this approach of cavity elongation raises a number of open questions regarding the retention of temporal coherence with increasing mode population, which is now known to lead to turbulence and a loss of coherence in a CW fiber system [4]. In this Letter, we present strong experimental and numerical evidence to support the fact that temporal coherence in an elongated fiber laser can be preserved up to cavities lengths in excess of 1 km, supporting over 10^6 interacting modes. Specifically, consideration is given to a recently demonstrated laser system, with a time-bandwidth product of 236—approximately 750 times the transform limit—generating pulses with a duration of 1.7 ns [8,9]. Although there are many alternative routes to generating nanosecond-scale optical pulses, we consider the dynamics of nanosecond mode-locked lasers here due to their fundamental intrinsic interest.

Three main findings are presented: (1) it is demonstrated, for the first time, that these highly chirped dissipative solitons are truly viable solutions of the relevant propagation equations, propagate coherently, and are completely distinct from the noise-burst operation observed in other mode-locked laser systems [10], which is in strong agreement with experimental evidence [9]; (2) it is found that the initial temporal intensity envelope, which emerges during the formation of these bright dissipative solitons, consists of many randomly formed and distributed dark soliton-like structures; and (3) these can persist for many hundreds of times the nonlinear length, implying partial self-organization. The existence of dark soliton-like features within a broader pulse envelope in dissipative soliton lasers is not a new phenomenon, having been identified in simulations reported in [11]. Importantly, however, such structures have previously only appeared in the unstable transition toward chaos, not during the asymptotic evolution of a stable attractor, and not as quasi-stationary solutions.

The following numerical model describes the experimental system reported in [8,9]. Briefly, it is a unidirectional ring laser consisting of a 2 m Yb-doped fiber amplifier, passively mode-locked by a fast saturable absorber. The cavity includes a 15% output coupler and a 1200 m length of passive optical fiber. Both passive and active fiber segments have a group velocity dispersion of $\beta_2 \sim 0.018$ ps^2 m^{-1} and a nonlinear coefficient of $\gamma \sim 0.003$ W^{-1} m^{-1}. The elongated cavity results in a total cavity dispersion of 21.6 ps^2.

The model is based on a modified scalar nonlinear Schrödinger equation (NLSE), augmented by a spectrally dependent gain term:

$$\partial_z \tilde{A}(z,\Omega) = i\frac{\beta_2}{2}\Omega^2\tilde{A}(z,\Omega) - \frac{\alpha(\Omega)}{2}\tilde{A}(z,\Omega) + i\gamma\mathcal{F}(A(z,\tau)|A(z,\tau)|^2) \quad (1)$$

with $\tilde{A}(z,\Omega)$ the Fourier transform of the complex field envelope $A(z,\tau)$, $\Omega = \omega - \omega_0$ the frequency with respect to the central pulse frequency ω_0, and $\tau = t - \beta_1 z$ the comoving frame, where β_1 is the inverse of the group velocity, related to the group index by the vacuum speed of light. The simulation field is represented on a temporal grid (and via the Fourier transform on a frequency grid) consisting of 2^{16} points, with a width of 6 ns.

We propagate the complex field sequentially through all cavity elements, iterating until a steady state is achieved, starting from an initial field equivalent to one photon per mode with random phase, as widely used in the simulation of other noise-driven nonlinear processes [12]. Higher-order dispersion, shock formation, and Raman terms were found to have no effect on the numerical results due to the limited spectral bandwidth of the output pulses. The gain of the Yb fiber was included through $\alpha(\Omega)$, with a parabolic gain bandwidth of 40 nm and peak gain given by $g = g_0/(1 + E/E_{\text{sat}})$, where $g_0 = 30$ dB is the small signal gain, and E and $E_{\text{sat}} = 200$ pJ are the input and input saturation energies of the amplifier, respectively. The absorption of the fast saturable absorber was modeled as $\alpha_{\text{SA}} = \alpha_{\text{S}}/(1+P/P_{\text{sat}}) + \alpha_{\text{NS}}$, with $\alpha_{\text{S}} = 0.05$ and $\alpha_{\text{NS}} = 0.45$ the saturable and nonsaturable absorptions, and P and $P_{\text{sat}} = 6$ W the input and saturation powers. The saturation power is representative of typical values for carbon-nanotube-based devices, as inferred directly by fitting data obtained through Z-scan characterization [13]. A Gaussian filter ($\Delta\lambda = 10$ nm), was applied in the frequency domain to represent the accumulated spectral filtering of all cavity components except the gain fiber. The round-trip loss was 3 dB, and the system was assumed to be linearly polarization maintaining.

Ensemble simulations of 1000 independent realizations, initiated from unique noise conditions, converged to a coherent attractor [see Figs. 1(a), 2(c), and 2(j)], with equivalent pulse width and energy. This is notable as these simulations represent the longest, purely normally dispersive cavity length modeled to date, by an order of magnitude, to permit coherent, single-pulse solutions [14]. Figure 1(a) shows the calculated spectrogram of the steady-state laser output. It can be seen that a single coherent pulse is the solution of the system, presenting no temporal fine structure within the pulse envelope, the signature of noise-like emission in a low-coherence regime [14]. In addition, it confirms that these pulses are highly chirped and correspond well with the previously reported analytical and experimental spectrograms [Figs. 1(b) and 1(c)], in [9]; briefly, the analytic result was computed using a form of the Haus master equation [15], while the experiment was performed using a monochromator in conjuction with a synchronously scanning streak camera.

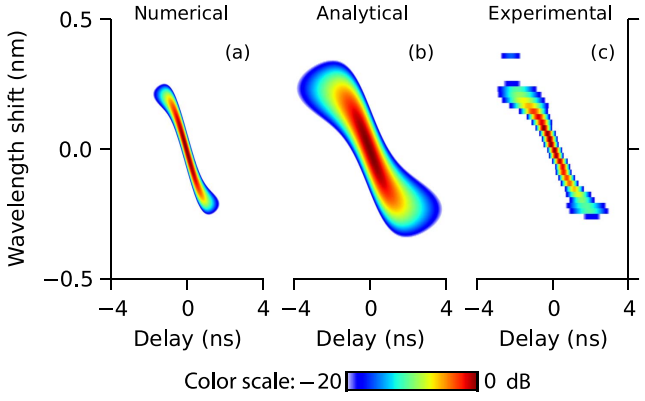

Fig. 1. Spectrograms of the steady-state output pulse at a center wavelength of $\lambda_c = 1065$ nm. (a) numerical, (b) analytical and (c) experimental after [9].

The dissipative soliton solutions of mode-locked fiber lasers that exhibit relatively large net normal dispersion have been called "giant-chirp oscillators" (GCOs) due to the large normal chirp they possess at the oscillator output [6]. While the compression of broadband pulses emitted from short-length GCOs is routine, there has been considerable controversy regarding the quality and coherence of the pulses from more extreme GCOs, where compression has proven experimentally intractable due to the extreme chirp of narrow band pulses [8,9]; in spite of the fact that these systems have been unequivocally demonstrated to generate pulses exhibiting predominantly quadratic and quartic chirp, with vanishing tertiary chirp, as should be expected from dissipative solitons [9]. The excellent agreement between experimental and numerical results shown in Fig. 1—as well as good agreement with the analytical solutions—strongly supports the extreme GCO hypothesis for ultra-long mode-locked fiber lasers.

Importantly, the numerical model can be used to probe the pulse-formation dynamics from an initial noise field to a coherent single pulse. Figure 2 shows the characteristic evolution of the temporal and spectral field intensity, with increasing numbers of round-trips of the resonant cavity: the top panel shows the temporal profiles; the bottom, the corresponding spectrum. It is clear that in the early stages of pulse formation the degree of pulse coherence is low [Fig. 2(a)], with a high density of subpulses within a broader pulse envelope; Fig. 2(d) shows the detail of this substructure. The corresponding spectrum [Fig. 2(h)] is broad with a domed top. This noisy-pulse behavior has been observed previously in partially mode-locked normally dispersive lasers, where clusters of modes form subpulses [16]. In the steady-state regime a single pulse exists, characterized by a sech^2-shaped temporal intensity profile [Fig. 2(c)] and a steep-edged spectrum [Fig. 2(j)]; such a pulse structure is predicted by analytic theory [9,15,17], and is commonly observed in laboratory experiments.

In the transition between a coherent single-pulse and a partially mode-locked noise burst, a phase exists in which isolated meta-stable dark—black (i.e., intensity drops to zero) and gray—pulses exist, as shown in Figs. 2(d) and 2(e). Plotting the phase across a typical black structure [Fig. 2(f)] reveals an abrupt phase step approximately equal to π, suggesting that the dark structures manifest as dark solitons [18]. To verify that the dark structures observed in Fig. 2 correspond to dark solitons, we fit them with their characteristic equation [18] and confirm that their width, τ_0, is commensurate with a fundamental black soliton solution through the soliton condition $|\beta_2|/\tau_0^2 = \gamma P_0$. We repeated this process for many of the black structures and always found good agreement; therefore we conclude that the dark pulses

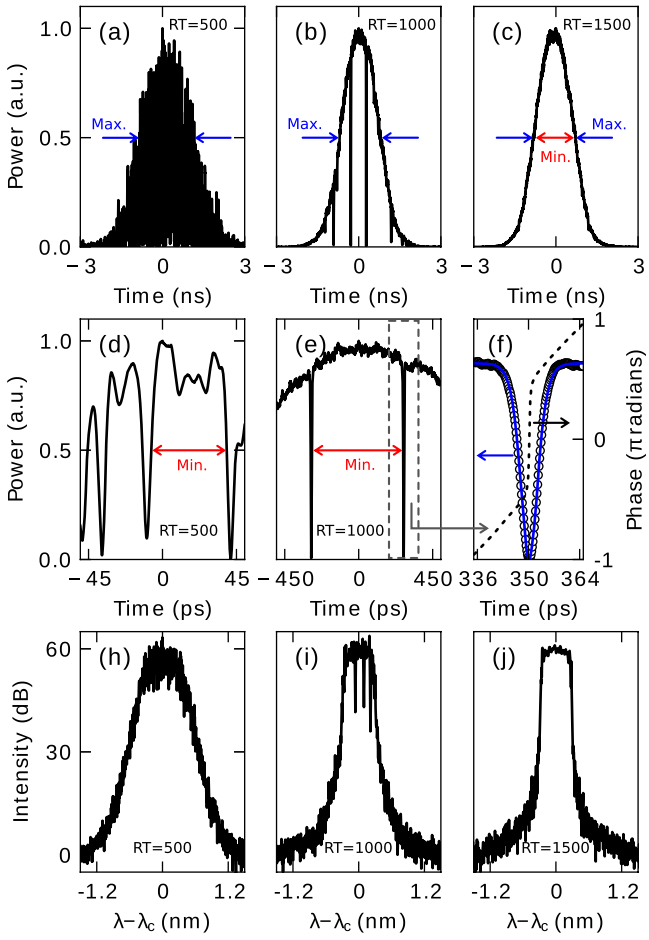

Fig. 2. Temporal [top, (a)–(c)], zoomed temporal [middle, (d), (e)], phase (f), and spectral [bottom, (h)–(j)] profiles for three different stages of the characteristic pulse evolution within the oscillator cavity. RT, round-trip number; min, internal pulse width; max, envelope duration. Center wavelength $\lambda_c = 1065$ nm.

in the early stages of the mode-locked pulse evolution in this system are in fact fundamental black solitons of the NLSE. This is remarkable, as they are stable within the nonconservative laser cavity over very many round trips. We note that these are distinct from the dark solitons previously discussed in the context of mode-locked fiber lasers, which were found as coherent and stable dissipative dark soliton solutions of the laser cavity [19–21]. The solitons found here evolve spontaneously from noise, propagate with a nonfixed velocity (due to the nonuniform background intensity), leading to soliton collisions, and eventually decay leaving a single bright dissipative soliton, with a much longer duration.

Figure 3(a) shows the spatiotemporal intensity evolution from noise to a coherent dissipative soliton. Dark components express themselves as gray/black trails with nonlinear trajectories, implying that their relative velocity is different from that of the pulse envelope. The three distinct pulsation regimes that form the evolution of the bright pulse can be clearly identified: (1) the noise-burst phase where partial mode-locking of modal clusters results in the development of a low coherence pulse with a broad envelope; (2) a region where accelerating picosecond-scale dark pulses can emerge from the noise structure and ultimately decay; and (3) the final asymptotic evolution toward a coherent bright pulse, with a duration on the nanosecond scale.

Multiple collision events between dark components lead to their rapid decay, evidenced by strongly curved (i.e., accelerating) trajectories in Figs. 3(a) and 3(b). Solitons on a sloping background intensity experience a phase modulation [18] and, given that the internal soliton phase determines its velocity, leads to a walk-off of the soliton relative to the group velocity at the center frequency of the background pulse.

Remarkably, under certain conditions, a dark soliton emerges from the noise that is located sufficiently close to the peak of the bright pulse, such that it experiences a near-uniform background intensity and can become meta-stable [18]. Figure 3(b) shows such a long-lived spatiotemporal feature that propagates stably for approximately 1000 iterations of the resonant cavity. Given the nonlinear length, $L_{\mathrm{NL}} = 1/\gamma P_0 \approx 2.4$ km, this feature persists for approximately $500 L_{\mathrm{NL}}$, implying it is quasi-stationary. While experimental observation of this phenomenon revealed by our simulations remains a

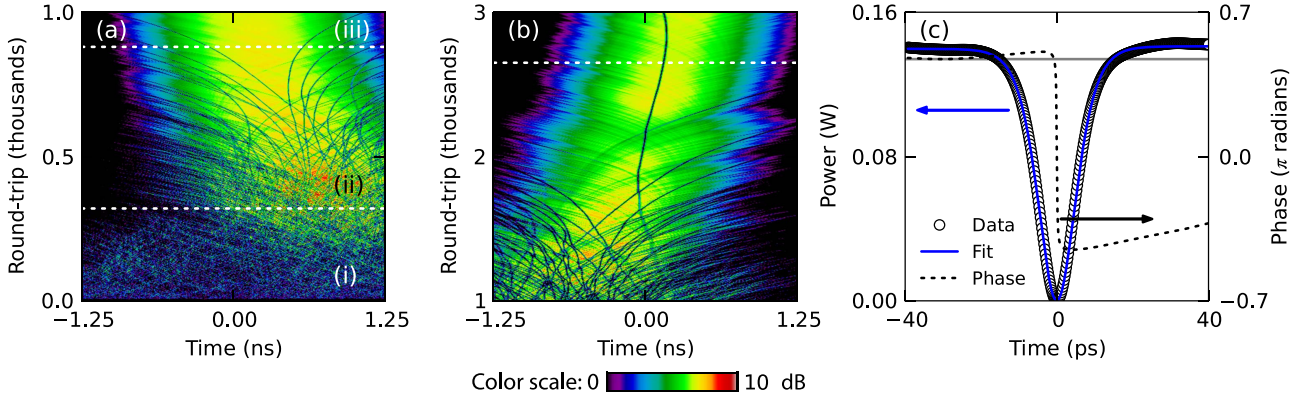

Fig. 3. (a) Spatiotemporal intensity evolution of a typical bright-pulse evolving from noise. Three distinct stages of pulse formation are identified (i, ii, iii); see text for a detailed description. (b) Spatiotemporal intensity evolution of an independent realization capturing a long-lived, quasi-stationary dark soliton. (c) Temporal intensity and phase slice, corresponding to the white dashed line in (b); the temporal phase shows an abrupt phase change approximately equal to π, across the black feature. The solid blue line is a fit to the functional form of a dark soliton [18], where $\tau_0 = 6.68$ ps corresponding to a background power of 0.134 W for a fundamental dark soliton (indicated by the solid gray line).

technical challenge, recent techniques for the single-shot characterization of ultrafast mechanisms involved in fiber-based supercontinuum [22], and the starting evolution of pulses in mode-locked fiber lasers [23] have emerged that could present a practical route; such approaches are being actively pursued.

In conclusion, highly chirped, bright dissipative soliton pulses can be the stable and coherent output of mode-locked fiber lasers with ultra-long cavities and strong normal dispersion. Numerical simulations that repeatedly converge to an equivalent coherent solution add to the comprehensive experimental evidence that nanosecond-scale mode-locked pulses are not incoherent bursts of noise. During the bright-pulse evolution, a large number of incoherent dark solitons spontaneously emerge from the initial noise and, subsequently, dephase due to acceleration and collisions caused by the nonuniform background and eventually decay, yielding a stable and coherent bright dissipative soliton pulse. Certain dark solitons can, however, exist for many thousands of cavity round-trips—many hundreds of times their nonlinear length—implying that they are quasi-stationary solutions of the system. Statistical analysis is needed to establish the likelihood of such phenomena; further study is required to establish the effect of cavity elongation that we predict plays an important role.

References

1. D. R. Solli, C. Ropers, P. Koonath, and B. Jalali, Nature **450**, 1054 (2007).
2. M. Erkintalo, J. M. Dudley, and G. Genty, Opt. Lett. **34**, 2468 (2009).
3. C. Lecaplain, Ph. Grelu, J. M. Soto-Crespo, and N. Akhmediev, Phys. Rev. Lett. **108**, 233901 (2012).
4. E. G. Turitsyna, S. V. Smirnov, S. Sugavanam, N. Tarasov, X. Shu, S. A. Babin, E. V. Podivilov, D. V. Churkin, G. Falkovich, and S. K. Turitsyn, Nat. Photonics **7**, 783 (2013).
5. A. Gordon and B. Fischer, Phys. Rev. Lett. **89**, 103901 (2002).
6. W. H. Renninger, A. Chong, and F. W. Wise, Opt. Lett. **33**, 3025 (2008).
7. S. Kobtsev, S. Kukarin, and Y. Fedotov, Opt. Express **16**, 21936 (2008).
8. E. J. R. Kelleher, J. C. Travers, Z. Sun, A. G. Rozhin, A. C. Ferrari, S. V. Popov, and J. R. Taylor, Appl. Phys. Lett. **95**, 111108 (2009).
9. E. J. R. Kelleher, J. C. Travers, E. P. Ippen, Z. Sun, A. C. Ferrari, S. V. Popov, and J. R. Taylor, Opt. Lett. **34**, 3526 (2009).
10. M. Horowitz, Y. Barad, and Y. Silberberg, Opt. Lett. **22**, 799 (1997).
11. A. Zaviyalov, O. Egorov, R. Iliew, and F. Lederer, Phys. Rev. A **85**, 013828 (2012).
12. J. M. Dudley and S. Coen, Opt. Lett. **27**, 1180 (2002).
13. J. C. Travers, J. Morgenweg, E. D. Obraztsova, A. I. Chernov, E. J. R. Kelleher, and S. V. Popov, Laser Phys. Lett. **8**, 144 (2011).
14. I. A. Yarutkina, O. V. Shtyrina, M. P. Fedoruk, and S. K. Turitsyn, Opt. Express **21**, 12942 (2013).
15. H. A. Haus, J. G. Fujimoto, and E. P. Ippen, J. Opt. Soc. Am. B **8**, 2068 (1991).
16. M. I. Dzhibladze, Z. G. Esiashvili, E. S. Teplitskii, S. K. Isaev, and V. R. Sagaradze, Sov. J. Quantum Electron. **13**, 245 (1983).
17. W. H. Renninger, A. Chong, and F. W. Wise, Phys. Rev. A **77**, 023814 (2008).
18. Y. S. Kivshar and B. Luther-Davies, Phys. Rep. **298**, 81 (1998).
19. H. Zhang, D. Y. Tang, L. M. Zhao, and X. Wu, Phys. Rev. A **80**, 045803 (2009).
20. S. Coen and T. Sylvestre, Phys. Rev. A **82**, 047801 (2010).
21. M. J. Ablowitz, T. P. Horikis, S. D. Nixon, and D. J. Frantzeskakis, Opt. Lett. **36**, 793 (2011).
22. D. R. Solli, G. Herink, B. Jalali, and C. Ropers, Nat. Photonics **6**, 463 (2012).
23. H. Li, D. G. Ouzounov, and F. W. Wise, Opt. Lett. **35**, 2403 (2010).